Accepted Manuscript

Biogeochemical anomaly response of circumboreal shrubs and juniper to the Juomasuo hydrothermal Au-Co deposit in northern Finland

Maarit Middleton, Johanna Torppa, Piippa R. Wäli, Raimo Sutinen

PII: S0883-2927(18)30260-9

DOI: 10.1016/j.apgeochem.2018.09.006

Reference: AG 4174

To appear in: *Applied Geochemistry*

Received Date: 23 April 2018

Revised Date: 3 September 2018

Accepted Date: 5 September 2018

Please cite this article as: Middleton, M., Torppa, J., Wäli, P.R., Sutinen, R., Biogeochemical anomaly response of circumboreal shrubs and juniper to the Juomasuo hydrothermal Au-Co deposit in northern Finland, *Applied Geochemistry* (2018), doi: 10.1016/j.apgeochem.2018.09.006.

Biogeochemical anomaly response of circumboreal shrubs and juniper to the Juomasuo hydrothermal Au–Co deposit in northern Finland

Maarit Middleton[1a], Johanna Torppa[2], Piippa R. Wäli[3], Raimo Sutinen [1]

[1a]Geological Survey of Finland, P.O. Box 77, 96101 Rovaniemi, Finland; maarit.middleton@gtk.fi, tel. +358295034345; corresponding author

[1]raimo.sutinen@gtk.fi; tel. +358295034303

[2]Geological Survey of Finland, P.O. Box 1237, 70211 Kuopio, Finland; johanna.torppa@gtk.fi; tel. +358295033271

[3] Unit of Ecology and Genetics, University of Oulu, P.O. Box 8000, FI-90014 University of Oulu, Finland; tel. +358407268137; piippa.wali@oulu.fi

Key words: Biogeochemistry, mineral exploration, common juniper, crowberry, Labrador tea, gold, cobalt

Abstract

Tree tissue chemistry has proven successful in guiding advanced exploration in the early stages of mineral exploration projects in Arctic and subarctic regions. In this paper, the biogeochemical response of three circumboreal shrubs, crowberry (*Empetrum nigrum* L.), Labrador tea (*Ledum palustre*) and bilberry (*Vaccinium myrtillus* L.), and one conifer, common juniper (*Juniperus communis* L.), to the underlying hydrothermal Juomasuo Au–Co deposit was assessed in southeast Finnish Lapland. A variety of contrasting spatial multi-elemental anomaly patterns were found for the elements Au and Co, along with Fe, Th, U and rare earth elements, such as Ce, La and Nd, in different plant tissue types over the subcropping lodes and also deep (blind) mineralizations down to a depth of 200 m in two seasonally varying campaigns: in late summer (August) 2013 and early summer (June) 2014. Besides these elements verified by lithogeochemistry, Ag, Bi, Mo, Se, Te, W and Ni exhibited anomalous spatial patterns over the mineralization. Based on the Mann-Whitney-Wilcoxon test, the Au concentrations in twigs/stems of crowberry, bilberry, Labrador tea and common juniper over the mineralization were found to be higher than the background, but the evergreen species gave the most consistent response to the mineralization. This also applied to U, W and Mo, as well as Nd and several other rare earth elements. Using unsupervised clustering with self-organizing maps and k-means, the location of the underlying mineralized zones could be determined with high overall accuracy (70–90%). This indicates that the biogeochemical anomaly patterns over the Juomasuo sulphidic lodes are strong, and the deposit would have been detected from the biogeochemical data even without prior knowledge gained from a diamond drilling campaign. The sampled vascular species are widely distributed over the pan-Arctic and circumboreal terrains, thus demonstrating their considerable significance to mineral exploration for hydrothermal Au ores at northern latitudes.

1 Introduction

Plant tissues, soil organic matter, humus and peat have been used as substances for detecting geogenic and anthropogenic inputs in circumboreal terrains (Lounamaa, 1956; Langille and MacLean, 1976; Kozlov et al., 2000; Kovalevskii and Kovalevskaya, 1989; Reimann et al., 2007). Biogeochemical exploration, involving sampling and chemical analysis of plant tissues, has been a common practice in formerly glaciated terrains in boreal and Arctic climate zones of the US, Russia and Canada (Brooks, 1972; Kovalevsky, 1987; Dunn, 2007).

A number of studies have demonstrated that biogeochemistry is an effective exploration method, especially for Au (Cohen et al., 1987; Kovalevsky, 1987; Reading et al., 1987; Kovalevskii and Kovalevskaya, 1989; Rencz and Hall, 1992; Rogers and Dunn, 1993; Anand et al. 2007; Reid and Hill, 2010; Lintern et al., 2013).

In northern boreal forests, the majority of studies have been conducted on tree foliage or bark (Kovalevskii and Kovalevskaya, 1989; Dunn, 2007; Reimann et al., 2007). Trees are favoured over other species as geochemical sampling media because of their extensive root systems, which can 'pre-concentrate' elements, and because of the ease of sampling. To be of practical use in biogeochemical exploration, however, the selected species must have a broad geographic distribution and uniform local coverage over the studied site. Due to intensive forest management practices in Finland, mature trees of the same species, such as Norway spruce (*Picea abies* (L.) Karst), Scots pine (*Pinus sylvestris* L.), downy birch (*Betula pubescens* Ehrh.) or silver birch (*Betula pendula*), are not often available as a sampling medium for mineral exploration. Instead, common juniper (*Juniperus communis* L.; hereafter referred to as juniper), extending through the pan-Arctic and circumboreal forests (Adams et al., 2003), could be utilized. Crowberry (*Empetrum nigrum*; Popp et al., 2011), Labrador tea (*Ledum palustre*; Langille and MacLean, 1976; Pugh et al., 2002) and bilberry (*Vaccinium myrtillus* L.; Reimann et al., 2001) are also common circumboreal species. Even though the soil water content is one of the most critical drivers for plant species distributions (Sutinen et al., 2002), it has previously been demonstrated that crowberry and bilberry are practically independent of the soil water content in northern boreal forests (Salmela et al., 2001). The seasonal soil water content in pine-dominated forest sites is less than 27% in volume, whereas soils beneath spruce–downy birch stands frequently exceed full saturation (>44%), particularly after snowmelt (Sutinen et al., 2002). Therefore, crowberry and bilberry could be used across a variety of sites in Finland where forests are managed intensively. On the other hand, Labrador tea, which is often found on organic soils at lower latitudes, grows on dry heaths in the Arctic. Juniper is also a pan-Arctic species (Adams et al., 2003) and tends to cover a wide range of habitats, from almost bare rocks to glacial tills with different particle-size distributions. The life span of juniper may extend to several hundreds of years, and it bioaccumulates elements through the root zone and rhizosphere processes, hence being an important species for prospectivity mapping (Närhi et al., 2014).

In northern Fennoscandia, plant species such as juniper, crowberry, heather (*Calluna vulcaris*), mosses, lichens and birch have been investigated for their Au, Cu and rare earth element (REE) concentrations (Erämetsä and

Yliruokanen, 1971; Yliruokanen, 1975; Pulkkinen et al., 1989; Harju and Hulden, 1990). Juniper and crowberry were found to contain significant Au concentrations at a site currently known as the Pahtavaara gold mine area in the Central Lapland Greenstone Complex (Pulkkinen et al., 1989). Multi-element vascular plant geochemical analytics with inductively coupled mass spectrometry was used for the first time in Finland near the Suurikuusikko gold mine, where juniper was found diagnostic for Au (Närhi et al., 2014). Juniper foliage chemistry was also shown to be anomalous at an Au-REE prospect at Mäkärärova (Närhi et al., 2013).

Thus far, no systematic multi-metal investigations with common angiosperms, such as crowberry, Labrador tea and bilberry, have been conducted in the Fennoscandian subarctic to support biogeochemical exploration on exploration targets where forest management practices have recently been conducted. The aim of this study was to objectively assess the biogeochemical spatial anomaly patterns of these vascular plant species on subcropping and deep-seated blind mineralizations of the glacially buried Juomasuo Au–Co deposit in southeast Finnish Lapland. In addition, the effect of the timing of the sampling during the summer season on these anomaly patterns was assessed, and it was investigated whether these anomalies could be detected without any prior knowledge of the underlying lithogeochemistry.

2 Material and Methods

2.1 Juomasuo deposit

The Juomasuo deposit belongs to the Kuusamo volcano-sedimentary belt of an Early Proterozoic rift system in the Fennoscandian Shield (Pankka and Vanhanen, 1992; Fig. 1). Juomasuo is the largest of the known Au deposits in the area, comprising a number of closely spaced, steeply dipping lodes over 280 metres in length that strike northwest–southeast and plunge steeply to the south and the southwest. Juomasuo comprises one major and a number of smaller lodes controlled by a NW-trending fault crossing an axial culmination in a NE-trending anticline. Native Au is chiefly associated with Bi and Te minerals as inclusions in pyrite, cobaltite and uraninite, between silicates, and in tiny Au–Bi–Te-rich veinlets oriented parallel to foliation and enveloped by silicates. The lithogeochemistry of the drill core data, reported in Pankka and Vanhanen (1992), Vanhanen (2001) and Dragon Mining (2011), was used as background data to determine the exact location of the mineralized lodes and their elemental distributions (see location in Fig. 2a). From the perspective of geochemical exploration, the ore elements Au, Co, Cu, Nd and U, and the pathfinder elements As, Ba, Bi, Ce, Fe, K, La, Mo, Ni, Pb, S, Se, Te and Th are interesting. The mineralization is covered by 2−5-m-thick glacial sediments. During the summer of 2013, pH values from 5.0 to 5.7 were measured in the eluvial podzolic horizon on top of the mineralized zone (Rekilä, 2015).

[Figure 1]

The Juomasuo deposit is hosted by albitised, biotitised and sulphidised mafic volcanic rock and sericite quartzite (see Fig. 1; 2a). The gold mineralization occurs within a larger zone of sulphidised and sheared rocks surrounded by lithologies strongly altered in sodium metasomatism (Vanhanen, 2001). Au–Co lodes are associated with secondary sericitic (K-mica) hydrothermal alteration and subordinately with chlorite-biotite alteration (Vasilopoulos et al., 2016). REE-forming minerals are allanite, monazite and bastnaesite, which are associated with the Au–Co mineralization. Uranium primarily occurs as discrete grains of uraninite, which are sporadically located within the gold lodes and to a lesser extent with the cobalt mineralization (Dragon Mining, 2011).

[Figure 2]

2.2 Sampling

Vascular plants were sampled along a SW–NE-oriented 1.3-km-long transect over the Juomasuo deposit such that ten sampling points (from the total of 37 sampling stations) were targeted at the known Au–Co subcropping mineralized zones. The survey line also crossed blind lodes at depths of 40−60 and 150−200 m (Fig. 1, Fig. 2). The sample spacing was approximately 20 metres, with the exception of a gap located on a peat bog on the NE portion of the transect (see Fig. 2b between points 328 and 332). The glacial streamlined drumlin morphology in the area is, to a great extent, erosional (Sutinen et al., 2010). Hence, only minor fingerprinting of the Late Weichselian glaciogenic dispersal on the biogeochemistry may be anticipated.

Crowberry, Labrador tea, bilberry and juniper were selected as sample materials. No single tree species was available for sampling across the whole deposit because of the variable soil hydrological conditions and forest management practices. Mechanical site preparation, such as the ploughing applied at Juomasuo, tends to result in the leaching of nutrients from the reworked soil (Sutinen et al., 2006). Thus, the plant samples were collected between the ploughed tracks. An equal length criterion was used when sampling vascular plant foliage: 15−20 cm foliage samples of Labrador tea, 10−15 cm of bilberry, 7−10 cm of crowberry and 20 cm of juniper. The maximum twig diameter of 5 mm was also applied (see Dunn, 2007). The determination of growth years was beyond the scope of this work because it significantly slows the sampling process. Närhi et al. (2014) demonstrated that the stunted growth of juniper may cause false-positive anomalies when an equal length sampling criterion for foliage is applied. Samples were collected in a consistent way at all sites, wearing untreated leather gloves and cutting samples with stainless steel garden clippers into cotton bags, which were stored in a well-aerated dry place until they were transported to the laboratory for drying in an oven (40 °C, 24 hours) immediately after the sampling campaign had been completed. In the laboratory, foliage samples were separated into the plant pulp media of leaves/needles and twigs/stems (see Dunn 2007 for details). The impact of sampling time (see Schiller et al., 1973; Langille and Maclean, 1976; Stednick et al., 1987) was tested such that late-season samples were collected between 29 and 30 August 2013 and early-season sampling was conducted at the same sites between 9 and 13 June 2014. Juniper, however, was only sampled in 2014. The data were considered as a combination of 14 different *subdatasets*, each composed of the concentrations of the same plant species, organ and sampling year, because only these observations represent the same origin and circumstances, thus being comparable with each other (Table 1). The number of observations in a subdataset varied from 25 to 37 (see Table 1), because at many of the predesignated sample sites, only some of the selected species were abundant enough for sampling.

In the field, duplicate samples were collected at every tenth sampling point for evaluation of the field precision. Laboratory accuracy was tested with samples of standard reference materials (SRM; Colin Dunn Consulting Ltd, Sydney, Canada) of ashed Eucalyptus leaves (Western Australia, Ash-1), pine bark (Central BC, Canada, Ash-2), pine twigs (Ontario, Canada, V6a) and tree tops of black spruce (Manitoba, V8a), which were inserted in the plant analysis sequence of a large sample batch including samples from five other sampling sites not reported in this study (a total of 1111 samples in 2013 and 715 in 2014; see Torppa and Middleton, 2017, for details). Altogether, 4.9% (n = 55) of all tissue samples in 2013 and 10.5% (n = 75) in 2014 were standard reference material samples evenly distributed throughout the analysis sequence.

2.3 Chemical analyses

Plant samples were macerated in a Wiley cutting mill until they passed a 1-mm heavy-metal-free steel screen. Approximately 50 g of dried material was accurately weighed into glass beakers and ashed at 475 °C for a total of 24 hours (4-hour ramp from ambient temperature to 475 °C, 16 hours at 475 °C, then 4 hours of cooling). A 0.25-g aliquot of ash was digested in a 1:1:1 $HCl:HNO_3:H_2O$ mixture at 95 °C for 1 hour with a sample-to-acid ratio of 1:6. The element concentrations were determined with inductively coupled plasma mass spectrometry (ICP-MS) and optical emission spectrometry (ICP-OES) at the Acme Analytical Laboratories (Vancouver, Canada) along with milling and ashing. The analysis provided results for 64 elements, including REEs. The 2013 and 2014 samples were analysed as two separate batches within three months from sampling. The analytical and field data used in this paper are available in electronic format in Torppa and Middleton (2017).

2.4 Quality control and choice of elements

A total of 28 of the 64 analysed elements were subjected to further analysis (Table 1). The rest were excluded in the quality control phase due to high uncertainty or a high percentage of samples under the lower detection limit (<LDL) or exceeding the upper detection limit (>UDL), or because they did not show a spatial anomaly pattern. Hereafter, the 28 selected elements are categorized into ore elements, pathfinder elements and elements that, based on visual inspection, exhibited spatial anomaly patterns in biogeochemical data. The ore and pathfinder elements, besides U, Bi, La, Se, Te and Th, were mostly well below the LDL. Similarly, other elements that showed anomaly patterns included a few elements with a high number of <LDL samples. However, all the elements that were included in further data analysis had at least 77.8% >LDL concentrations for at least one species. Ashing preconcentrated the contents of the major plant elements K, Mn and P beyond the sensitivity range of instrumentation calibrations (see Torppa and Middleton, 2017). These elements should thus be analysed from dried and milled samples.

The quality of the data was assessed in terms of laboratory accuracy, precision and contamination, as well as field precision (see comprehensive results in Torppa and Middleton, 2017). Laboratory accuracy was defined by computing the mean and standard deviation for the concentrations of standard reference material samples analysed in the course of the project (Sec 2.2) and comparing them with their expected values provided along with the SRMs. Laboratory and field precision were evaluated by computing the relative difference (D%) between the concentrations of each sample pair of laboratory and field duplicates, respectively, as

$$D\% = \frac{c_1 - c_2}{\bar{c}},$$

where c_1 and c_2 are the concentrations of the duplicate pair components and $\bar{c}$ is the mean of c_1 and c_2. The average D% of field duplicates (Table 1) mostly exceeded 30%, but was below 20% for Al, Cu, Fe, Ni, S and Ti, which can be considered as the most accurate elements, since their laboratory accuracy was also good at typical project sample concentrations. The effect of laboratory contamination was assessed by measuring concentrations in blank samples. For the majority of the elements, contamination was negligible, but Fe appears to have been somewhat prone to sporadic contamination. A significant proportion of the blank samples had Fe concentrations up to 15% of the typical project sample concentrations.

2.5 Data pre-processing

Concentrations in ash obtained from the laboratory (c_{ash}) were converted to dry weight concentrations (c_{dry}) to enable comparison with the results of future studies. Due to improved detection limits, most modern vegetation analysis is conducted on dry tissue. The conversion was carried out by multiplying each sample concentration with the sample ash yield: c_{dry} = y*c_{ash}, where the ash yield (y) is the ratio between the ashed sample weight and the dried sample weight. Samples with concentrations <LDL and >UDL were retained in the dataset, but their dry weight concentrations were set to a predefined constant value to make them separable from other samples. Under the LDL values were first set to half of the LDL and then multiplied by the minimum ash yield of all of the <LDL samples, whereas >UDL concentrations were increased by 20% and then multiplied by the maximum ash yield of all the UDL samples of the particular subdataset. Total light rare earth elements (LREE: La, Ce, Pr, Nd, Sm, E, Gd) and heavy rare earth elements (HREE: Y, Tb, Dy, Ho, Er, Tm, Yb, Lu) often included elements with concentrations <LDL (Table 1). If HREE or LREE elements with concentrations <LDL represented more than 20% of the total HREE or LREE concentration of a sample, the total concentration was considered as <LDL, and was given a constant value (sum of the lower detection limits of the HREE or LREE constituent elements). This was to mimic the datasets of the individual elements, for which samples with a concentration <LDL were also given a single value, as described above. Concentrations exceeding the UDL were not observed for REEs.

2.5 Data analysis

Besides visual exploratory data analysis presence and contrast of the biogeochemical anomaly patterns at Juomasuo were evaluated with three approaches to test whether biogeochemical data can be used to detect the presence of known underlying mineralized lodes: 1) The Mann-Whitney-Wilcoxon (MWW) test was used to check whether single element concentrations on and off the deposit differ from each other in a statistical sense, 2) response ratios (RR) were computed to be able to compare the anomalies in different subdatasets and 3) data clustering was carried out to find groups of samples with a similar chemical composition. In this paper, only the essential findings of the study are presented, while a complete report of the results for all the elements and all the species in the form of graphs and tables is provided by Torppa & Middleton (2017).

Significance of the anomalies (MWW test)

To test whether the element concentrations above the mineralization differ in a statistical sense from the background concentrations, the sampling points were divided into two categories based on the known Juomasuo lithology derived from drill core analysis: the *on-deposit* category included samples taken directly above the subcropping mineralization and the mineralized lodes at depth (40−60 m and 150−200 m; sample numbers 320, 329, 330, 331, 337, 339, 340, 342, 345 and 346), while the *background* samples included all the samples outside the mineralized zones (see Figs 1 and 2a). The distributions of the on-deposit and background categories were compared using the non-parametric Mann-Whitney-Wilcoxon test (MWW, e.g., Mann and Whitney, 1947) with the null hypothesis stating: “The distributions of the two compared sample sets, on the top of the mineralization and in the background, represent the same distribution.” The tests were performed using the R function wilcox.test (R Development Core Team, 2012).

Response ratios

To be able to compare the strength of anomalies along the sampling transect for different elements, species and organs, the response ratio (RR) was computed. The RR relates each sample concentration to a selected background value. The median of the lowest quartile of the distribution for the particular element and dataset in question was used as the background value. The RR_i for sample i was computed as

$$RR_i = \frac{c_i}{\mathrm{MED}(\boldsymbol{Q1})},$$

where c_i is the concentration of the i^{th} sample, vector $\boldsymbol{Q1}$ contains the concentrations below the first quartile, and MED refers to the median. In addition to studying the contrast for each subdataset and element, the RRs were plotted for each subdataset one element at a time on line plots with distance between points on the x-axis for visual inspection of the anomaly patterns.

Unsupervised clustering

The unsupervised multidimensional clustering method SOM was used to investigate how a suite of elements behaved spatially in the study area and whether the biogeochemical anomaly patterns would have revealed the underlying mineralization without prior knowledge of it. SOM (Kohonen, 2001) is a neural-network-type clustering method that simultaneously performs clustering and dimension reduction without any assumption regarding the form of the data distribution or the relationships within the subdataset. Clustering was accomplished using the two-level approach described in Vesanto and Alhoniemi (2000): pre-clustering with SOM followed by further clustering with k-means (hereafter referred to as *SOMKm*). No specific number of clusters was fixed for the k-means clustering, but the solution with the smallest Davies-Bouldin (DB) index was chosen. The DB index is defined as

$$DB = \frac{1}{N}\sum_{i=1}^{N} \max_{j \neq i} \frac{S_i + S_j}{M_{i,j}},$$

where N is the number of clusters, S_i is the scatter within cluster i, and $M_{i,j}$ is the distance between the centroids of clusters i and j. Thus, the smaller the scatter within the clusters and the larger the distance between the cluster centroids, the smaller is the DB index.

However, if the variation in the DB index was small, 2 to 4 clusters were preferred. The CSIRO SOMKm implementation SiroSOM was used (CSIRO, 2018; Bierlein et al. 2008). The aim of the unsupervised multidimensional clustering with SOMKm was to demonstrate how well a selected combination of elements can be clustered to distinguish the samples on the deposit from the background. To replicate a real-world scenario of mineral exploration without *a priori* knowledge of the underlying lithogeochemistry, only the elements that displayed a clear spatial anomaly pattern (based on RR line plots) in most subdatasets, i.e. Au, Ce, Co, Fe, La, Nd, Th and U, were selected as inputs.

The success of SOMKm clustered biogeochemistry in revealing the known underlying mineralized lodes at the

Juomasuo deposit was evaluated using the overall accuracy (OA) values calculated as OA = (TP+TN)/N, where TP is the number of true positives, TN is the number of true negatives assigned by SOMKm clusters and N is the total number of data points (Congalton, 1991). The same division of the sampling points into the on-deposit class and background class (see Figs 1 and 2a) as in MWW was used as with positive and negative samples. The OA computation and final division of SOMKm clusters into positive and negative classes was carried out in several steps for each subdataset. First, each SOMKm cluster in turn was set as the trial positive class, while the other clusters were set to represent the background, and the corresponding OA was computed for each SOMKm cluster. Secondly, the clusters were ranked according to OA. Then, two to three clusters in the order of decreasing OA were combined, set as the trial positive class, and the corresponding OA was computed. The final division into positive and negative classes was chosen as the division that provided the best OA.

3 Results and discussion

3.1 General levels of element concentrations

The median elemental concentrations (in dry weight) for the plant species and their organs along the entire sampling transect are listed in Table 1. A complete table of statistical parameters is provided in Torppa and Middleton (2017). Significant differences in concentration levels between the sampled species and their organs were evident. For example, juniper had higher contents of Co, La, Ni and Te compared to other species. Overall, leaves had higher concentrations than twigs for all species except juniper, in which needles had lower concentrations than its twigs. Information on the differences in concentration levels will be relevant to practical exploration in the future when selecting species and their tissue types in cases where the concentrations are close to the LDL.

The statistics can also be used to compare the concentrations in the study area with concentrations elsewhere and thus evaluate whether the overall concentrations at the sampling site are indicative of the underlying mineralization. Overall concentrations across the entire Juomasuo site compared to sampling sites and different species over deposits elsewhere in northern Finland (compared to statistics presented in Torppa and Middleton, 2017) were slightly higher for Ba, Mo, Nd, Th, U and W. However, the commodity elements Au, Co and Cu were not elevated. Elevated contents of Mo, Nd, Th, U and W could be related to the underlying lithogeochemistry, but elevated Ba could not be verified with the available lithogeochemical data. When the concentrations in ash were compared with previous studies, the Co concentration in bilberry (0.098 µg/kg) was twice as high as that in bilberry and crowberry (0.044−0.051 µg/kg) measured throughout northern Europe (Reimann et al., 2001). The highest measured concentrations of Au in juniper twigs were up to 44 µg/kg (in ash) over the Juomasuo lodes. These figures are rather similar to those of up to 54 µg/kg in juniper foliage at the Suurikuusikko shear zone reported by Närhi et al. (2013), but minor compared to those (up to 70 µg/kg) reported by Pulkkinen et al. (1989) over the Sattasvaara volcanic complex in central Finnish Lapland. The plants applied in this study were common pan-Arctic and circumboreal species that are not hyperaccumulators or metallophytes (see Brooks, 1972).

In target-scale exploration, concentration levels are generally less important than spatial anomaly patterns (compare Sec 3.2; see Dunn, 2007). The Juomasuo case demonstrates that elevated concentrations of ore or pathfinder elements may provide an additional indication of the presence of a metallogenic region, and comparison with concentrations in other datasets may act as an additional data interpretation key. Although the hypothesis could not yet be tested, the generally elevated levels of certain elements may also provide an opportunity to apply biogeochemistry in regional-scale exploration. It remains unclear why concentrations of the commodity elements Au, Co and Cu were not higher than in other biogeochemical datasets over different types of mineralization in northern Finland, or why they were considerably lower compared to the biogeochemical dataset over Au deposits (Pulkkinen et al., 1989; Närhi et al., 2013). Explanations may be found in the complex interactions of element phytoavailability and uptake by plants (see e.g. Kabata-Pendias, 2001; Reimann et al., 2015; Pedziwiatr et al., 2018).

[Table 1]

3.2 Spatial anomaly detection

The p-values of the MWW test, tabulated in Table 2, illustrate that the on-deposit and background samples had statistically significant differences in the distribution of element contents in every subdataset for several ore and pathfinder elements. The concentrations of a long list of additional elements on the deposit also differed from the background concentrations ($p < 0.05$), which supports the general interpretation of the biogeochemical data

(Dunn, 2007) that it is not only the ore and pathfinder elements, often verified by the lithogeochemistry of diamond drillings, that are important in the interpretation of biogeochemical exploration data.

In Figure 3, examples of line plots for the response ratios along the sampling transect for selected elements and subdatasets are presented. In these examples, the mineralized lodes at different depths (150−200 m, 40−60 m and subcropping) caused visually clear spatial patterns in the biogeochemical subdatasets, as also demonstrated by the MWW statistical analysis (Table 2). Compared to the subcropping lodes and lodes lying at the depth of 40−60 m, the mineralized lode at the depth of 150−200 m caused a weaker biogeochemical response. In addition, there were only two observation points representing the deep-lying lode (for more data, see Torppa and Middleton, 2017). The anomaly patterns are noisy, i.e. containing non-contrasting observations from the background merely caused by factors such as spatial variation in the underlying lithogeochemistry and inconsistencies in the biogeochemical sampling material (e.g. age, genetic variation).

[Figure 3]

In Table 3, the maximum RR values for major and minor plant nutrients in the Juomasuo subdatasets are also presented (see also Torppa and Middleton, 2017). It was observed that the maximum RRs along the sampling transect were low, and especially low for major and minor plant nutrients. This indicates that the contrast in the Juomasuo biogeochemical data is rather low compared, for example, to the leach of mobile metal ions in soil calculated similarly to Mann et al. (1998), among others. The intake of major and minor nutrients is especially controlled by plants, causing their lower contrast compared to other elements and low RRs compared to soils (see e.g. Reimann et al., 2015). Our results demonstrate, however, that the contrast with the background does not have to be large in order for an anomaly to be significant when detecting an underlying deposit. The observations also emphasize the importance of using plant trace elements in anomaly interpretation when conducting biogeochemical mineral exploration. In the Juomasuo case, the main commodity elements, Au and Co, exhibited high RRs (RR > 10) on the mineralization for most of the plant species. Trace elements displayed highly varying RR values, with the maximum values concentrated in, but not restricted to, the on-deposit samples.

The overall accuracies of the unsupervised SOMKm indicate very successful separation of the ‘anomaly’ from the ‘background’ (Table 4). The overall accuracies (OA, Sec. 2.5) of single SOMKm clusters and their combinations for all 14 subdatasets are presented in Table 4. Cluster 1 itself usually shows the presence of underlying mineralized zones, with high OAs between 70−90% (Clusters 1–6). OAs for cluster 2 are also acceptable if the classification has three or more classes varying between 53−77% AO. The combination of clusters 1 and 2 (Table 4, Cluster 1+2) gives almost equal OAs (63–83%) to Cluster 1. The examples in Figure 3 demonstrate that the background samples were most often contained within a single cluster, while the samples above the mineralization fell in two or three clusters. The results of the SOMKm analysis confirm that the anomalies in the Juomasuo biogeochemical data are pronounced and underlying mineralization would therefore have been detected even without prior knowledge of it.

[Table 4]

The line plots in Figure 3 confirm the MWW and SOMKm results, illustrating that for many of the sampled species, tissue types and elements, the spatial anomaly patterns are very local (see also Torppa and Middleton, 2017). Pervasive hydrothermal alteration, more specifically sodium metasomatism, and the following sequence of alteration events has depleted the surrounding schist belt rocks to form the Juomasuo deposit, causing a steep lithogeochemical gradient between the mineralization and surrounding rocks (Vanhanen, 2001). It is speculated that the main reason for the extremely clear biogeochemical anomalies is the underlying geology, but also the very weak hydromorphic dispersion due to the underlying well-drained glacial sediments. Some weakly dispersed anomalies can, however, be observed. In our experience, there has been no other reported case study in Finland in which the anomalies have equally contrasted with the background in biogeochemical data and have appeared in several plant species and for a large number of elements.

SOMKm, or a similar unsupervised clustering method, can therefore be seen as a valuable tool for increasing confidence in anomaly interpretation in cases such as Juomasuo, where many of the elements produce observable anomalies. One cluster may already indicate the location of the mineralization, but care has to be taken in the interpretation of unsupervised clusters, and visualization of the elemental concentrations within the clusters could be further developed. The application of SOMKm should be tested for a variety of datasets before further conclusions are drawn, but it can be expected that the use of suitable multivariate numerical data analysis methods will provide complimentary information to visual inspection and increase the efficiency of geochemical data analysis.

The vicinity of the dust sources i.e. the test pit and the gravel road and the drill sites (Fig. 2) raised a concern of potential contamination by airborne dust and soya from bedrock drilling. We assessed the spatial patterns of ash yield and dust indicating elements such as Fe, Al and high field strength elements and ore forming elements spatially overlaid them with in GIS data and drill sites. We cannot completely exclude the contamination from these sources but conclude that the anomalies have to be dominantly geogenic because the anomaly patterns are highly local to underlying mineralized lodes.

3.3 Selection of sampling material

The results of the Mann-Whitney test and SOMKm clustering suggest that Labrador tea, crowberry and juniper are feasible materials for the detection of the mineralized lodes in Juomasuo. Based on the MWW results, crowberry and Labrador tea twigs and their leaves, as well as juniper twigs, were able the separate the on-deposit samples from the background samples for the largest number of elements (Table 2). In addition, the highest SOMKm OA of 90% was calculated for the late season 2013 Labrador tea twig subdataset (Table 4). These species displayed several element anomalies, implying that the confidence level when using these species in mineral exploration is high. Conversely, bilberry twigs and leaves and juniper needles were rather poor indicators for many elements, forming spatial anomaly patterns for only a few elements. The SOMKm OA values are in agreement with the MWW p-value (Table 2), suggesting that the most successful clustering to separate the deposit from the background was achieved with crowberry and Labrador tea subdatasets. On the other hand, juniper needle data from 2014 clustered well, although only three elements yielded p-values below 0.05. Therefore, the evergreens are concluded to be more diagnostic of the underlying lithogeochemistry than the annually leaf shedding bilberry. In addition, the evergreen dwarf shrubs and juniper are feasible materials for sampling at different times of year. For crowberry, bilberry and Labrador tea, there is no significant difference depending on whether leaves or twigs are used (Table 2; 4). Juniper twigs distinguished the on-deposit observations from the background slightly better than needles according to the MWW test (Table 2).

3.4 Seasonal variation

The elemental concentration levels not only varied between the species and plant organs, but also seasonally (Table 1). Concentrations for almost all elements are higher in the June 2014 (early season) data compared to the August 2013 data (late season). The finding is consistent with the observation of Dunn (2007) that concentrations peak in the early summer and then decline towards the late summer. Similarly, Langille and Maclean (1976) found Co and Mo concentrations in Labrador tea and bilberry to be higher in spring (April) compared to summer (July) in Nova Scotia, Canada. At Juomasuo, contrastingly, some elements had higher contents in the late season compared to the early season. For example, the late season Ag contents were higher than the early season ones in all species and plant organs, the only exception being Labrador tea leaves, for which the figures were rather similar (Table 2). Similarly, the highest Au contents were recorded in the late season crowberry leaves and stems, as well as the late season Labrador tea stems and leaves. The concentrations of As, Ba, Mo, Na, Ni, Pb, Sc and particularly Cu were higher in the early season in bilberry leaves. However, the element concentrations in the evergreens, such as crowberry, appear to be less seasonally controlled.

Although seasonal differences in concentration levels are evident, they do not have an effect on the detection of the anomaly patterns at Juomasuo. According to the MWW (Table 2) and SOMKm results (Table 4), no significant difference was observed between the early and late season efficiencies in distinguishing the on-deposit from the background samples (Table 2). For the radiogenic elements U and Th in all materials (twigs, leaves, needles) and species, the on-deposit samples could be distinguished from the background samples regardless of the sampling season, indicating their stability in plant tissues. The Juomasuo study highlights that in the case of strong multi-element biogeochemical anomaly patterns, it is not critical to sample during the growing period for successful detection of an underlying mineralization.

4 Conclusions

A biogeochemical orientation survey was repeated with the pan-Arctic and circumboreal shrubs crowberry (*Empetrum nigrum* L.), Labrador tea (*Ledum palustre*), bilberry (*Vaccinium myrtillus* L.) and common juniper (*Juniperus communis*) over the glacially buried Juomasuo Au–Co deposit in northern Finland in two consecutive years with 20-m sample spacing. The geochemical response over the deposit observed in plant chemistry was very local and strong: the anomalies were multi-elemental and were observed in all the sampled species and their organs. Most significantly, mineralized zones at different depths, including subcropping and deep-seated lodes (at depths of 40−60 m and 150−200 m), produced biogeochemical anomalies. The extraction of major and minor elements from the soil is a complex process with several interactions between the soil pH, microorganisms and plant root systems. However, the biogeochemical signatures in the tested shrubs and juniper on the deposit, as compared to background concentrations, provide a basis to spatially outline the underlying hydrothermally altered deposits in northern Fennoscandia. It is speculated that the main reason for the clear local anomaly patterns at Juomasuo is the strong lithologically controlled contrast of the mineralization with the background and the reducing soil conditions over the sulphidic mineralized lodes. Strong alteration of sodium metasomatism (Vanhanen, 2001) in the surroundings of the Juomasuo deposit has depleted the host rocks of elements that are enriched to the ore lodes.

The Juomasuo case study highlights the following interpretation principles relevant in biogeochemical mineral exploration:

1) Target-scale mineral exploration can be highly successful with shrubs such as crowberry and Labrador tea and with common juniper, and intermediate with bilberry. In advanced exploration stages of Juomasuo-type orogenic Au deposits, sampling of the first three abovementioned species is highly recommended to complement the conifer tree biogeochemistry.
2) Concentration levels of Ba, Mo, Nb, Th, U and W were found to be much higher in most sampled materials compared to samples taken over other types of prospects in northern Fennoscandia. Although biogeochemical exploration merely consists of spatial anomaly detection, comparison of the concentration levels may provide a clue to the presence of a larger metallogenic region and act as an additional key to the interpretation of biogeochemical data.
3) Besides the main commodity elements Au and Co, the elements Al, As, Ce, Co, Cr, Fe, La, Mo, Na, Nd, Sc, Th, Ti, U, V, W, Y, HREE and LREE were also able to distinguish the mineralization from the background, emphasizing the use of pathfinder elements and the testing of a wide spectrum of elements in laboratory analysis.
4) The contrast between the on-deposit and background samples, quantified by response ratios, was low, especially for major and minor plant elements. The statistical analyses, however, demonstrated that the

Juomasuo mineralized lodes could still be detected in the data, emphasizing the significance of low contrasting biogeochemical anomalies from a mineral exploration perspective.

5) Unsupervised clustering with self-organizing maps and k-means (SOMKm) using visually selected elemental data also revealed the location of the mineralization. SOMKm could aid in data interpretation by increasing the confidence in anomaly detection, but should never be applied blindly without careful selection of the input elements.
6) Evergreens were found to be more diagnostic of the underlying Au–Co deposit than the annually leaf shedding bilberry. Crowberry twigs were the most efficient plant tissues for revealing the location of the mineralized lodes.
7) The concentrations of the majority of the elements and sampling media were higher in the early-season 2014 data compared to the late-season 2013 data. However, there was no difference in how successfully the spatial anomaly patterns were revealed by subdatasets from different sampling seasons, indicating that strong biogeochemical anomalies are detectable throughout the summer season.
8) Since the biogeochemical anomaly patterns were found to be very local and undispersed, biogeochemical greenfield exploration of these spatially fragmented Au–Co deposit types might not be as successful on a regional scale unless the sample spacing is <<50 m. The key to successful geochemical characterization of the targets is an adequate sampling density and careful selection of the sampling locations.

5 Acknowledgements

This paper presents findings from two projects: 1) the UltraLIM project (Ultra low-impact exploration methods in the subarctic, 2013−2015), financed by the Green Mining programme of Tekes (the Finnish Funding Agency for Technology and Innovation, currently known as Business Finland) and mining companies (AA Sakatti Mining, Pyhäsalmi Mine, First Quantum Minerals, Dragon Mining, Agnico-Eagle Finland, Finnish Forest and Parks Service), and 2) the UpDeep project (Upscaling deep buried geochemical exploration techniques into European business, 2017−2020), funded by European Information and Technology Raw Materials. Discussions with Colin Dunn significantly improved the paper. Olli Pajula and Pentti Grönholm from Dragon Mining kindly provided expertise and interpretation of the bedrock lithogeochemistry for this work, and Jyrki Bergström assisted in the sampling design. The fieldwork and laboratory assistance of Päivi Heikkilä, Paula Haavikko, Elisa Kyllönen, Olli Junttila, Paavo Närhi, Janne Rekilä and Markku Virtanen, as well as editorial help from Pertti Turunen, Pertti Telkkälä and Viena Arvola are greatly appreciated. Kent Middleton and Roy Siddall revised the language.

6 References

Adams, R.P., Pandey, R.N., Leverenz, J.W., Dignard, N., Hoegh, K., Thorfinnsson, T., 2003. Pan-Arctic variation in Juniperus communis: historical biogeography based on DNA fingerprinting. Biochemical Systematics and Ecology 31, 181−192.

Anand, R.R., Cornelius, M., Phang, C., 2007. Use of vegetation and soil in mineral exploration in areas of transported overburden, Yilgarn Craton, Western Australia: a contribution towards understanding metal transportation processes. Geochemistry: Exploration, Environment, Analysis 7, 267−288.

Bierlein, F., Fraser, S., Brown, W., Lees, T. 2008. Advanced methodologies for the analysis of databases of mineral deposits and major faults, Australian Journal of Earth Sciences, 55 (1), 79−99.

Brooks, R.R., 1972. Geobotany and Biogeochemistry in Mineral Exploration. Harper & Row, New York.

Cohen, D.R., Hoffman, E.L., Nichol, I., 1987. Biogeochemistry: A geochemical method for gold exploration in the Canadian Shield. Journal of Geochemical Exploration 29, 49−73.

Congalton, R.G., 1991. A review of assessing the accuracy of classifications of remotely sensed data. Remote Sensing of Environment 37 (1), 35−46.

CSIRO, 2018. SiroSOM self organising maps: complex datasets made simple. Available at: https://www.csiro.au/en/Research/MRF/Areas/Data-driven-mining-decisions/Self-organising-maps. (Accessed 23rd August, 2018).

Dragon Mining 2011. Electronic resource. Available at http://www.dragon-mining.com.au/exploration/finland-kuusamo

Dunn, C.E., 2007. Biogeochemistry in mineral exploration. Elsevier, Amsterdam.

Harju, L., Huldén, S-G., 1990. Birch sap as a toll for biogeochemical prospecting. Journal of Geochemical Exploration 37, 351−356.

Erämetsä, O., Yliruokanen, I., 1971. The rare earths in lichens and mosses. Suomen Kemistilehti B44, 121−128.

Kabata-Pendias, A., 2001. Trace elements in soils and plants, third ed. CRC Press, Boca Raton.

Kohonen, T., 2001. Self-organizing maps. Third Extended Edition, Springer Series in Information Sciences 30. Springer-Verlag, Berlin.

Kovalevskii, A.L., Kovalevskaya, O.M., 1989. Biogeochemical haloes of gold in various species and parts of plants. Applied Geochemistry 4, 369−374.

Kovalevsky, A.L., 1987. Biogeochemical exploration for mineral deposits. VNU Science Press, Utrecht.

Kozlova, M.V., Haukioja, E., Bakhtiarov, A.V., Stroganov, D.N., Ziminac, S.N., 2000. Root versus canopy uptake of heavy metals by birch in an industrially polluted area: contrasting behaviour of nickel and copper. Environmental Pollution 107 (3), 413−420.

Langille, W.M., MacLean, K.S., 1976. Some essential nutrient elements in forest plants as related to species, plant part, season and location. Plant and Soil 45, 17−26.

Lintern, M., Anand, R., Ryan, C., Paterson, D., 2013. Natural gold particles in Eucalyptus leaves and their relevance to exploration for buried gold deposits. Nature Communications 4. Electronic resource. Available at doi:10.1038/ncomms3614.

Lounamaa, J., 1956. Trace elements in plants growing wild on different rocks in Finland: A semi-quantitative spectrographic survey. Annals of the Botanical Society and Zoology botany of Fennoscandia, Vanamo 29, 196.

Mann, H.B., Whitney, D.R., 1947. On a Test of Whether one of Two Random Variables is Stochastically Larger than the Other. Annals of Mathematical Statistics 18 (1), 50–60.

Mann, A.W., Birrell, R.D., Mann, A.T., Humphreys, D.B., Perdrix, J.L., 1998. Application of the mobile metal ion technique to routine geochemical exploration. Journal of Geochemical Exploration 61(1–3), 87–102.

Närhi, P., Middleton, M., Sutinen, R., 2013. Gold prospectivity of common juniper and Norway spruce in Suurikuusikko shear zone, Finnish Lapland. Journal of Geochemical Exploration 128, 80−87.

Närhi, P., Middleton, M., Sutinen, R., 2014. Biogeochemical multi-element signatures in common juniper at Makärärova, Finnish Lapland: Implications for Au and REE exploration. Journal of Geochemical Exploration 138, 50−58.

Pankka, H.S., Vanhanen, E.J., 1992. Early Proterozoic Au-Co-U mineralization in the Kuusamo district, northeastern Finland. Precambrian Research 58, 387−400.

Pędziwiatr, A., Kierczak, J., Waroszewski, J., RatiéCécile, G., Quantin, C., Ponzevera, E., 2018. Rock-type control of Ni, Cr, and Co phytoavailability in ultramafic soils. Plant Soil 423, 339−362.

Popp, M., Mirré, V., Brochmann, C., 2011. A single Mid-Pleistocene long-distance dispersal by a bird can explain the extreme bipolar disjunction in crowberries (Empetrum). PNAS 108, 6520−6525.

Pugh, R.E., Dick, D.G., Fredeen, A.L., 2002. Heavy metal (Pb, Zn, Cd, Fe, and Cu) contents of plant foliage near the Anvil Range lead/zinc mine, Faro, Yukon Territory. Ecotoxicology and Environmental Safety 52, 273−279.

Pulkkinen, E., Räisänen, M.-L., Ukonmaanaho, L., 1989. Geobotanical and biogeochemical exploration for gold in the Sattasvaara volcanic complex, Finnish Lapland. Journal of Geochemical Exploration 32, 223−230.

R Development Core Team, 2012. R: A language and environment for statistical computing. R Foundation for Statistical Computing, Vienna. http://www.R-project.org/.

Reading, K.A.L., Brooks, R.R., Naidu, S.D., 1987. Biogeochemical prospecting for gold in the Canadian Arctic. Journal of Geochemical Exploration 27, 143−155.

Reid, N., Hill, S.M., 2010. Biogeochemical sampling for mineral exploration in arid terrains: Tanami Gold Province, Australia. Journal of Geochemical Exploration 104, 105−117.

Reimann, C., Arnoldussen, A., Boyd, R., Finne, T.E., Koller, F., Nordgulen, Ø., Englmaier, P., 2007. Element contents in leaves of four plant species (birch, mountain ash, fern and spruce) along anthropogenic and geogenic concentration gradients. Science of the Total Environment 377, 416−433.

Reimann, C., Englmaier, P., Fabian K., Gough, L., Lamothe, P., Smith, D., 2015. Biogeochemical plant-soil interaction: Variable element composition in leaves of four plant species collected along a south-north transect at the southern tip of Norway. Science of the Total Environment 506-507, 480−495.

Reimann, C., Koller, F., Frengstad, B., Kashulina, G., Niskavaara, H., Englmaier, P., 2001. Comparison of the element composition in several plant species and their substrate from 1 500 000-km2 area in Northern Europe. Science of the total Environment 278, 87−112.

Rekilä, J., 2015. Heikkouuttomenetelmien käyttö malminetsinnässä Kuusamon Juomasuolla Koillismaalla (in Finnish). Unpublished Master’s thesis, University of Oulu, 76 p., 16 appendixes. Electronic publication, available at http://jultika.oulu.fi/Record/nbnfioulu-201511172151.

Rencz, A.N., Hall, G.E.M., 1992. Platinum group elements and Au in arctic vegetation growing on gossans, Keewatin District, Canada. Journal of Geochemical Exploration 43, 265−279.

Rogers, P.J., Dunn, C.E., 1993. Trace element chemistry of vegetation applied to mineral exploration in eastern Nova Scotia, Canada. Journal of Geochemical Exploration 48, 71−95.

Salmela, S., Sutinen, R., Sepponen, P., 2001. Understorey vegetation as an indicator of water content in till soils in Finnish Lapland. Scandinavian Journal of Forest Research 16, 331−341.

Schiller, P., Cook, G.B., Kitzinger-Skalova, A., Woifl, E., 1973. The influence of seasonal variation for gold determination in plants by neutron activation analysis. Radiochemical and Radioanalytical Letters 13, 238−286.

Stednick, J.D., Klem, R.B., Riese, W.C., 1987. Temporal variation of metal concentrations in biogeochemical samples over the Royal Tiger mine, Colorado, part I: Within year variation. Journal of Geochemical Exploration 28, 75−88.

Sutinen, R., Teirilä, A., Pänttäjä, M., Sutinen, M-L., 2002. Distribution and diversity of tree species with respect to soil electrical characteristics in Finnish Lapland. Canadian Journal of Forest Research 32, 1158−1170.

Sutinen, R., Pänttäjä, M., Teirilä, A., Sutinen, M-L., 2006. Effect of mechanical site preparation on soil quality in former Norway spruce sites. Geoderma 136, 411−422.

Sutinen, R., Hyvönen, E., Närhi, P., Haavikko, P., Piekkari, M., Middleton, M. 2010. Sedimentary anisotropy diverges from flute trends in south-east Finnish Lapland. Sedimentary Geology 232, 190−197.

Torppa, J., Middleton, M., 2017. Biogeochemical data analysis methods and R implementation in the UltraLIM project. Geological Survey of Finland, GTK archive report 8/2017, 31 p., attachment file UltraLIM_biogeochem.zip. Electronic resource. Available at http://tupa.gtk.fi/raportti/arkisto/8_2017.pdf.

Vanhanen, E., 2001. Geology, mineralogy and geochemistry of the Fe-Co-Au-(U) deposits in the Paleoproterozoic Kuusamo Schist Belt, northeastern Finland. Geological Survey of Finland, Bulletin 359, 229 p.

Vasilopuolos, M., LeFèbre, M., Molnár, F., Richard, A., Andre-Mayer, A-S., 2016. Hydrothermal alteration and sources of fluids in the Juomasuo Au-Co deposit, Kuusamo Schist Belt, Finland. In: Staboulis, S., Karvonen, T., Kujanpää, A. (eds) Abstracts of The 32nd Nordic Geological Winter Meeting, 13th−15th January 2016, Helsinki, Finland. Bulletin of the Geological Society of Finland, Special Volume, p. 119. Electronic resource. Available at http://www.geologinenseura.fi/bulletin/Special_Volume_1_2016/BGSF-NGWM2016_Abstract_Volume.pdf.

Vesanto, J. and Alhoniemi, E., 2000. Clustering of the self-organizing map. IEEE transactions on neural networks 11 (3), 586−600.

Yliruokanen, I., 1975. Uranium, thorium, lead, lanthanoids and yttrium in some plants growing on granitic and radioactive rocks. Bulletin of the Geological Society of Finland 47, 71−78.

Figure and table captions

Figure 1. Lithological cross-section of the Juomasuo Au–Co deposit and surroundings in Kuusamo, Finnish Lapland. The 3D interpretation and drawing of the cross-section was based on drill core data (grey lines). Sampling points are marked with crosses (see location in Fig. 2) and drill holes with light grey lines (R77-R191).

Figure 2. a) Plant sampling points on top of a false-colour composite of an aerial photograph (© National Land Survey of Finland). The sampled species were not present on the peatland, resulting in an unsampled section of the sampling transect between points 328 and 332. b) Sampling points on top of the surface projection of the lithological interpretation of Figure 1.

Figure 3. Example line plots of the early season 2014 biogeochemical data. In figures a–d, spatial anomaly patterns along the Juomasuo sampling transect are expressed as response ratios. The sample colour coding is based on five quantiles to make the samples comparable across the plot. Missing observations are shown as black dots. Blue = deep mineralization (depth 150−200 m), green = deep mineralization (depth 40−60 m) and red = subcropping lodes. In the second set of line plots (e–h), spatial anomaly patterns are expressed as dry weight concentrations. The self-organizing maps and k-Means (SOMKm) clusters are given in numbers and

explained in Table 3. HREE is the sum of heavy rare earth elements.

Table 1. Lower detection limits (LDL, in ash), percentage of observations under the LDL (%<LDL), field precision (of field duplicate pairs) as the relative difference (D%), laboratory accuracy as the relative standard deviation (RSD) and the bias of inserted standard reference materials in concentration units (according to 2013 sampling), and the median concentration (dry weight) for selected elements for the sampled plant species and organs along the sampling transect on the Juomasuo Au–Co deposit and at background sites. The median concentrations are illustrated as bars for visual effect and the bars are scaled according to the element. The number of samples (n) for each sampling material is also given. Only elements verified from lithogeochemistry or having anomalous spatial patterns in the biogeochemical data are presented. For additional statistical tables, see Torppa and Middleton (2017).

Table 2. The p-values for the Mann-Whitney-Wilcoxon test of the null hypothesis that the distribution of on-deposit sample concentrations does not deviate from the distribution of background sample concentrations in the plant organs on the Juomasuo Au–Co deposit. Late-season samples were collected in August 2013 and early-season samples in June 2014. Cells with p-values >0.05 are coloured in white, i.e. the null hypothesis of equal distributions for the on-deposit and background samples is not rejected. Cells with p-values ≤0.05 are coloured with grey, denoting that the distributions differ significantly, with the on-deposit concentrations being greater than the background concentrations. Only elements verified from lithogeochemistry or having anomalous patterns in the biogeochemical data are presented.

Table 3. Maximum response ratios (RR) for a subdataset (the same species, tissue type and sampling year) for plant macronutrients, micronutrients and selected other relevant elements. Unlike other tables in this article, all plant micro and macronutrients are presented. To ease visualization, the background of the cells is grey scaled from low RRs (white) to high RRs (dark grey).

Table 4. Overall accuracy (OA) values for the individual SOMKm clusters (Class1–6) and their combinations (Class1+2 etc.) considering the ability to separate the deposit from the background. For the accuracy of the combined clusters, individual clusters were first ranked according to their OA and then combined in the order of decreasing OA. The selection of elements was based on visual interpretation of the spatial anomaly patterns and

included Au, Ce, Co, Fe, La, Nd, Th and U for all plant species and organs. The text colours correspond to the cluster colours in Fig. 3.

							crowberry				bilberry				L. tea				juniper	
				Field	Lab	Lab	2013	2014	2013	2014	2013	2014	2013	2014	2013	2014	2013	2014	2014	
Element	Unit	LDL	%<LDL	prec.	RSD	bias	twig		leaf		twig		leaf		twig		leaf		twig	needle
n							30	36	30	36	29	37	29	37	27	36	28	36	25	25
Ore elements				D%	%	%	median													
Au	µg/kg	0.2	11.6	90.5	56.9	30.8	0.0823	0.0324	0.0843	0.0155	0.0426	0.039	0.0608	0.0256	0.0794	0.0408	0.077	0.0583	0.0441	0.0386
Co	mg/kg	0.1	0.0	28	13.7	6.1	0.0635	0.0593	0.0769	0.0759	0.0809	0.0592	0.0852	0.0437	0.0579	0.0468	0.0475	0.0479	0.23	0.336
Cu	mg/kg	0.01	0.0	12	6.8	5.6	4.92	5.18	4.5	4.16	5.65	4.89	3.89	9.17	3.86	3.9	4.47	4.17	3.07	2.37
Nd	mg/kg	0.02	1.1	44.5	11.2	9.6	0.00561	0.0118	0.0129	0.0197	0.00485	0.00628	0.00909	0.0135	0.0112	0.0124	0.012	0.0198	0.0298	0.0258
U	mg/kg	0.1	38.3	34	15.3	21.8	0.00112	0.00427	0.00028	0.00383	0.000281	0.00247	0.000281	0.00028	0.0027	0.0038	0.0028	0.0051	0.00302	0.00028
Pathfinder elements																				
As	mg/kg	0.1	13.4	77.5	28.2	20.7	0.00958	0.0182	0.0251	0.0221	0.0126	0.0166	0.000281	0.0225	0.0178	0.0194	0.007	0.0248	0.0231	0.0163
Ba	mg/kg	0.5	0.0	38	11.9	11.4	3.01	5.45	27.4	26.2	4.26	17	36.1	37.2	8.39	7.78	18.2	33.1	32.2	27.5
Bi	mg/kg	0.02	42.9	48	33.6	22.4	0.00066	0.00113	0.00095	5.52E-05	5.62E-05	5.52E-05	5.62E-05	5.52E-05	0.0007	0.0011	0.0013	0.0013	0.00052	5.52E-05
Ce	mg/kg	0.1	0.0	26	14.6	12.4	0.0163	0.0315	0.0319	0.049	0.0158	0.0169	0.0248	0.0458	0.0269	0.0369	0.0336	0.0631	0.0846	0.0799
Fe	10 g/kg	0.01	5.7	20.5	26.8	19.5	0.00146	0.00222	0.00325	0.0042	0.00227	2.76E-05	0.00377	0.00428	0.0026	0.0023	0.0038	0.0038	0.00287	0.00462
La	mg/kg	0.5	25.6	31	13.6	12.3	0.00838	0.0169	0.0201	0.0285	0.00141	0.00138	0.00141	0.0191	0.0133	0.0176	0.0219	0.0305	0.118	0.113
Mo	mg/kg	0.01	0.0	36.5	21.5	8.8	0.0214	0.024	0.0458	0.0559	0.0412	0.0385	0.0866	0.116	0.0208	0.0175	0.0354	0.032	0.0208	0.0689
Ni	mg/kg	0.1	0.0	19	11.4	6.0	0.457	0.59	1.67	1.83	0.34	0.318	0.554	0.658	0.422	0.434	0.456	0.556	1.2	3.18
Pb	mg/kg	0.01	0.0	27.5	7.8	7.1	0.181	0.265	0.174	0.227	0.177	0.23	0.0911	0.224	0.251	0.267	0.13	0.245	0.231	0.143
S	10 g/kg	0.02	0.0	14	8.0	7.2	0.0242	0.029	0.0383	0.0327	0.0435	0.0372	0.0817	0.0846	0.0186	0.0159	0.0557	0.0344	0.0213	0.0201
Se	mg/kg	0.1	62.4	74	95.2	31.4	0.00213	0.00213	0.00664	0.000276	0.000281	0.000276	0.000281	0.00028	0.0041	0.0013	0.0017	0.0014	0.00028	0.00028
Te	mg/kg	0.02	41.5	88.5	128.8	11.8	5.62E-05	0.000457	5.62E-05	0.000827	5.62E-05	5.52E-05	0.000978	5.52E-05	0.001	0.0007	0.0003	0.0011	0.00154	0.00127
Th	mg/kg	0.1	39.5	28.5	27.9	10.6	0.00112	0.00375	0.0029	0.00527	0.000281	0.000276	0.000281	0.00368	0.0015	0.0029	0.0003	0.0055	0.00028	0.00329
Additional elements showing biogeochemical anomaly patterns																				
Ag	µg/kg	2	0.0	31.5	17.5	12.7	1.88	1.77	2.15	2.07	1.28	0.81	1.27	0.902	1.66	1.38	1.52	1.69	1.08	1.48
Al	10 g/kg	0.01	0.0	20.5	8.5	3.3	0.00123	0.00178	0.00304	0.00392	0.011	0.0106	0.0153	0.0109	0.002	0.0021	0.003	0.0051	0.0018	0.00212
Cr	mg/kg	0.5	0.9	28.5	16.4	2.2	0.0381	0.0836	0.0743	0.101	0.0319	0.0459	0.0391	0.0722	0.0546	0.0597	0.0851	0.135	0.088	0.0988
Na	10 g/kg	0.001	0.0	27	13.9	8.5	0.00228	0.0129	0.00242	0.00876	0.00274	0.01	0.00237	0.0157	0.002	0.0078	0.0023	0.016	0.00871	0.00668
Sc	mg/kg	0.1	22.4	44.5	15.3	6.9	0.00328	0.00164	0.018	0.0272	0.00252	0.000276	0.0158	0.0211	0.0045	0.0056	0.0133	0.03	0.0103	0.00028
Ti	10 g/kg	0.001	2.9	15	9.3	11.0	0.0003	0.000378	0.00056	0.000688	0.000459	0.000412	0.000407	0.00104	0.0003	0.0003	0.0005	0.0008	0.00041	0.00064
Tl	mg/kg	0.02	44.2	33.5	23.3	6.5	0.00096	5.52E-05	0.00147	5.52E-05	0.0032	5.52E-05	0.00145	5.52E-05	0.0219	0.0013	0.161	0.0029	5.52E-05	5.52E-05
V	mg/kg	2	29.3	36	26.3	5.0	0.0441	0.0629	0.0312	0.0983	0.0758	0.00552	0.0843	0.00552	0.0507	0.0975	0.0911	0.249	0.101	0.00552
W	mg/kg	0.1	18.1	47.5	31.1	43.9	0.00568	0.00631	0.00604	0.0079	0.00542	0.00486	0.000281	0.00356	0.0073	0.0059	0.006	0.006	0.00601	0.00658
Y	mg/kg	0.01	0.0	31	10.5	7.8	0.00303	0.00613	0.00767	0.01	0.00378	0.00455	0.00702	0.0092	0.0061	0.0074	0.007	0.0127	0.0179	0.0222
HREE	mg/kg						0.00589	0.00999	0.0133	0.0173	0.000478	0.00743	0.0112	0.0156	0.0115	0.012	0.0109	0.0191	0.0267	0.0333
LREE	mg/kg						0.034	0.0652	0.0837	0.124	0.0259	0.00215	0.0556	0.0969	0.0607	0.0784	0.084	0.153	0.27	0.235

	crowberry				bilberry				L. tea				juniper	
	2013	2014	2013	2014	2013	2014	2013	2014	2013	2014	2013	2014	2014	2014
Ore elements	twig		leaf		twig		leaf		twig		leaf		twig	needle
Au	0.21	0	0.18	0.44	0.35	0	0.12	0.39	0	0	0.03	0.01	0.01	0.34
Co	0.02	0	0	0	0.12	0.07	0.31	0.1	0	0	0	0	0.02	0.06
Cu	0.25	0.86	0.84	0.95	0.87	0.71	0.67	0.35	0.02	0.49	0.82	0.72	0.94	0.8
Nd	0	0	0	0	0	0	0	0.43	0.02	0	0	0	0.05	0.07
U	0	0	0	0	0.01	0	0.01	0.01	0	0	0	0	0	0.04
Pathfinder elements														
As	0.02	0	0.06	0	0.11	0.23	0.09	0.01	0.04	0	0.01	0	0.1	0
Ba	0.04	0.06	0.07	0	0.51	0.11	0.27	0.97	0.08	0	0.92	0.38	0.04	0.11
Bi	0.01	0.31	0.58	1	0.67	0.56	0.15	0.77	0.88	0.92	0.86	0.74	0.43	1
Ce	0	0	0	0	0	0	0.04	0.17	0	0	0	0	0.06	0.04
Fe	0	0	0	0	0	0.98	0.11	1	0	0	0	0	0	0.1
La	0	0	0	0	0.1	0	0.03	0.65	0	0	0	0	0.18	0.15
Mo	0.03	0.01	0.04	0.01	0.37	0.14	0.26	0.1	0.04	0	0.02	0	0.45	0.72
Ni	0.01	0.16	0.14	0.32	0.67	0.9	0.49	0.77	0.71	0.95	0.42	0.18	0.01	0.11
Pb	0.33	0.26	0.73	0.93	0.39	0.67	0.26	0.88	0.99	0.89	0.89	0.38	0.89	0.83
S	0.37	0.16	0.98	0.43	0.41	0.78	0.74	0.06	0.87	0.81	0.8	0.67	0.27	0.7
Se	0.54	0.08	0.05	0.02	0.15	0.06	0.22	0.08	0.56	0.19	0.14	0.16	0.13	0.38
Te	0.76	0.03	0.7	0.98	0.04	0.79	0.57	0.08	0.02	0.02	0.73	0.45	0.38	0.09
Th	0	0	0	0	0.34	0.02	0.03	0.13	0	0	0	0	0	0.01
Additional elements showing biogeochemical anomaly patterns														
Ag	0.05	0.15	0.11	0.16	0.03	0.22	0.03	0.77	0.13	0.19	0.53	0.05	0.42	0.13
Al	0	0	0	0	0.27	0.01	0.21	0.37	0	0	0	0	0.01	0.02
Cr	0	0	0	0	0.05	0	0	0.86	0.03	0	0	0	0	0.01
Na	0.11	0	0	0	0.08	0.03	0.43	0.34	0.04	0.02	0.53	0.04	0.04	0.49
Sc	0.01	0	0	0	0.63	0.66	0.79	0	0.04	0	0	0	0.03	0.38
Ti	0.01	0	0	0	0.08	0.03	0.49	0.6	0.01	0	0.12	0	0	0.12
Tl	0.08	1	0.95	0.77	0.04	0.91	0.01	1	0	0	0	0	0.51	1
V	0	0	0	0	0.09	0.04	0.05	0.99	0.05	0.01	0	0.29	0.05	0.29
W	0.01	0	0	0	0.04	0	0.15	0.01	0.01	0	0.01	0	0	0.02
Y	0	0	0	0	0	0	0.01	0.81	0	0	0	0	0.05	0.06
HREE	0	0	0	0	0.02	0	0.05	0.81	0	0	0	0	0.04	0.07

LREE	0	0	0	0	0.01	0	0.04	0.16	0	0	0	0	0.11	0.13

	crowberry				bilberry				L. tea				juniper		
	2013	2014	2013	2014	2013	2014	2013	2014	2013	2014	2013	2014	2014	2014	all
Major nutrients	twig		leaf		twig		leaf		twig		leaf		twig	needle	datasets
Ca	1.6	1.6	1.4	1.6	1.7	1.6	1.3	1.4	1.6	1.4	1.3	1.4	2.4	1.9	2.4
K	1.0	1.0	1.0	2.9	1.0	1.0	1.0	1.0	1.0	1.0	1.0	1.0	4.4	3.0	4.4
Mg	1.6	1.4	1.3	1.4	1.4	1.6	1.6	1.6	1.7	1.6	1.4	1.4	1.9	1.8	1.9
Mn	1.0	1.0	1.0	1.0	1.0	1.0	1.0	1.0	1.0	1.0	1.0	1.0	4.4	6.6	6.6
P	9.2	8.9	1.4	1.4	1.3	1.4	1.5	1.0	10.3	8.1	4.5	3.8	2.1	1.9	10.3
S	1.4	1.5	2.4	1.6	1.6	2.1	2.5	2.3	1.8	1.4	1.4	1.5	1.6	2.1	2.5
Minor nutrients															
B	1.7	1.9	2.0	2.0	1.4	1.3	1.9	2.0	1.5	2.4	1.6	1.7	4.5	1.7	4.5
Co	24.0	23.0	13.4	12.1	10.6	14.9	9.8	11.4	13.9	11.6	8.0	9.6	5.5	5.6	24.0
Cu	1.3	1.4	1.6	1.6	1.5	1.5	1.9	1.4	1.8	1.6	1.4	1.6	1.6	2.0	2.0
Fe	5.7	7.3	3.5	5.2	2.1	71.6	1.9	3.0	4.2	6.3	2.7	6.4	6.7	2.8	71.6
Zn	1.9	1.6	2.2	2.0	1.6	1.7	2.3	1.4	1.8	1.5	1.9	1.8	1.6	1.6	2.3
Others															
Ag	18.1	31.7	28.9	39.0	14.9	6.6	10.0	24.8	31.0	11.2	31.0	5.0	25.5	18.3	39.0
Al	4.6	6.3	2.7	3.7	1.6	1.7	2.1	1.6	2.6	4.2	2.6	3.8	3.1	3.1	6.3
As	510.4	13.5	55.3	16.3	337.6	10.9	234.0	7.5	65.0	19.8	982.0	12.2	46.1	435.7	982.0
Au	10.3	14.2	31.8	831.8	9.4	8.8	39.1	401.6	47.4	32.5	69.9	8.3	11.4	298.2	831.8
Ba	12.6	9.6	1.7	1.7	2.2	9.6	7.2	2.8	37.7	21.7	8.2	8.3	9.9	7.5	37.7
Bi	29.9	47.0	48.7	79.5	20.1	33.0	75.4	32.3	6.7	5.1	94.0	3.0	42.9	1.0	94.0
Ce	5.0	10.7	3.9	7.4	3.4	3.3	2.7	1.9	3.9	6.3	3.1	7.4	8.8	6.0	10.7
Cr	13.7	8.3	6.9	7.8	7.9	3.0	4.6	2.2	6.8	7.4	5.0	6.3	4.2	3.6	13.7
La	5.0	10.1	34.8	7.5	15.2	17.5	16.8	22.9	3.3	7.9	28.5	8.3	27.2	285.5	285.5
Mo	10.8	29.7	14.3	101.7	25.2	8.8	26.0	17.4	30.6	7.9	21.5	15.2	17.4	137.6	137.6
Na	2.8	2.2	2.3	4.4	1.9	1.8	3.4	1.8	2.2	3.3	3.1	3.4	3.3	2.1	4.4
Nd	8.6	10.0	4.4	7.8	5.5	4.1	5.5	1.9	4.0	8.3	6.1	9.3	6.7	7.6	10.0
Ni	2.1	1.8	1.8	1.9	2.3	2.0	1.7	2.1	2.6	2.5	2.2	1.8	4.5	4.3	4.5
Pb	2.4	3.7	2.3	2.4	1.9	2.3	2.2	2.3	2.1	1.9	1.8	2.0	2.3	1.9	3.7
Sc	39.9	141.6	9.2	13.4	32.3	37.7	3.8	2.2	10.7	8.7	2.9	3.5	4.6	62.2	141.6
Se	54.9	44.7	85.4	27.5	26.9	31.2	82.4	41.9	69.7	91.7	83.2	61.4	28.9	14.6	91.7
Te	47.2	55.3	87.1	71.9	141.8	53.5	222.4	104.5	114.8	63.5	125.4	155.4	55.8	59.2	222.4
Th	25.2	13.3	45.5	15.1	9.5	20.0	16.8	27.8	26.7	14.2	35.6	11.9	34.6	33.3	45.5
Ti	3.0	3.0	2.7	2.6	2.0	1.4	255.5	1.5	1.9	2.3	1.5	2.5	2.3	2.2	255.5

Tl	7.6	1.0	8.2	9.4	8.2	26.0	90.0	1.0	13.2	22.6	5.6	12.2	66.0	1.0	90.0
Tm	1.0	10.4	1.0	24.0	1.0	1.0	1.0	1.0	3.4	8.7	1.0	19.4	1.0	1.0	24.0
U	71.6	116.3	184.6	454.4	1314.7	436.3	790.7	166.6	117.4	17.0	70.5	10.1	135.3	99.8	1314.7
V	6.7	7.7	30.0	6.9	2.3	16.6	34.1	38.3	4.1	4.7	34.1	114.9	3.1	23.3	114.9
W	32.8	114.4	785.5	201.0	182.1	339.8	440.6	452.1	35.5	12.2	507.1	7.1	196.8	258.2	785.5
Y	5.0	9.3	5.0	7.3	3.5	3.0	3.9	1.7	3.3	7.9	4.2	7.6	5.9	8.2	9.3
HREE	41.0	10.0	4.9	7.9	27.4	30.5	73.4	1.9	3.0	9.4	67.4	8.9	117.7	166.2	166.2
LREE	5.2	10.7	4.8	7.5	2.2	2.7	2.3	1.7	3.7	7.1	3.4	7.0	12.5	21.6	21.6

			Individual clusters						Combination of two clusters					
			Cluster 1	Cluster 2	Cluster 3	Cluster 4	Cluster 5	Cluster 6	Cluster 1+2	Cluster 1+3	Cluster 2+3	Cluster 1+4	Cluster 2+4	Cluster 3+4
crowberry	2013	twig	0.87	0.73	0.17				0.83	0.27	0.13			
	2014		0.78	0.76	0.19				0.81	0.24	0.22			
	2013	leaf	0.80	0.77	0.20				0.80	0.23	0.20			
	2014		0.81	0.73	0.70	0.19			0.81	0.78	0.70	0.27	0.19	0.16
bilberry	2013	twig	0.77	0.77	0.77	0.73	0.23							
	2014		0.78	0.73	0.19				0.81	0.27	0.22			
	2013	leaf	0.83	0.53	0.37				0.60	0.43	0.13			
	2014		0.70	0.68	0.65	0.65	0.59	0.54						
L. tea	2013	twig	0.90	0.57	0.33				0.63	0.40	0.07			
	2014		0.73	0.24										
	2013	leaf	0.87	0.70	0.20				0.77	0.27	0.10			
	2014		0.81	0.73	0.14				0.84	0.24	0.16			
juniper	2014	twig	0.76	0.73	0.65	0.54			0.49	0.41	0.38	0.30	0.27	0.19
	2014	needle	0.84	0.65	0.49				0.49	0.32	0.14			

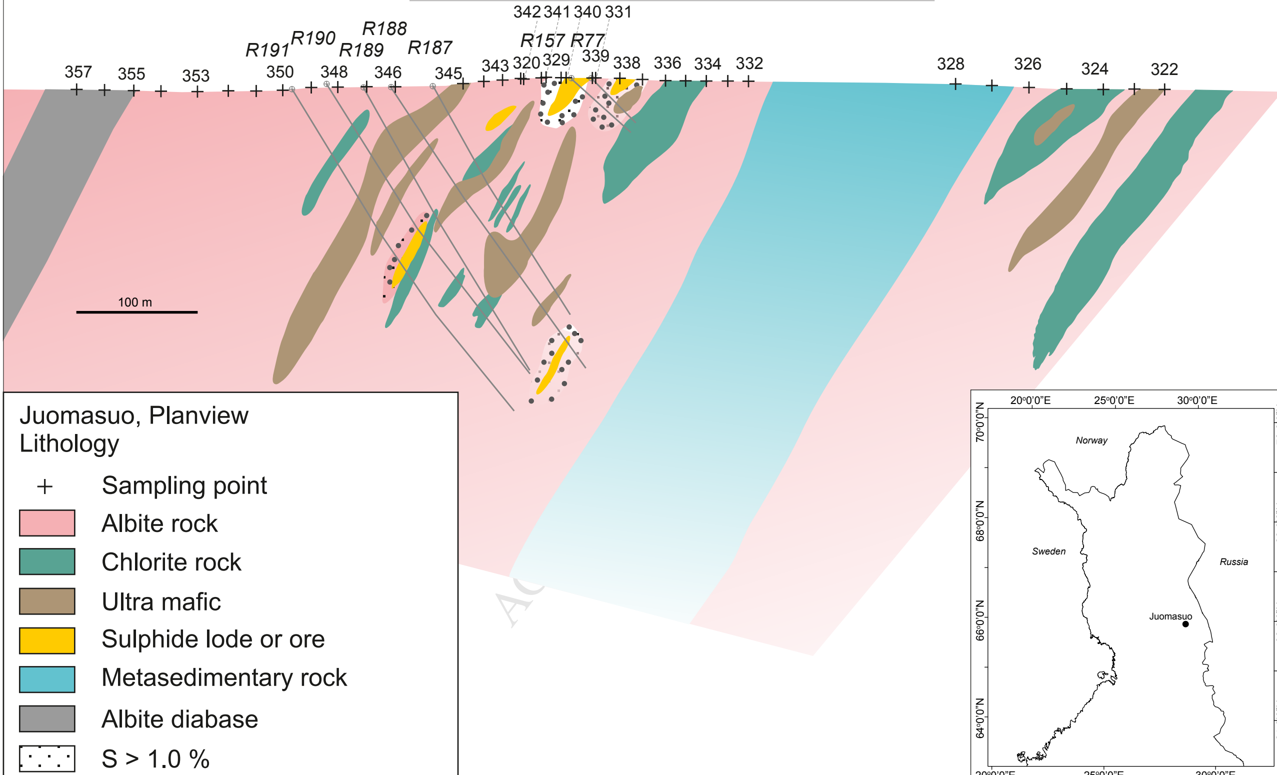

342 341 340 331
R188
R191 R190 R189 R187
R157 R77
357 355 353 350 348 346 345 343 320 329 339 338 336 334 332 328 326 324 322
30
110
190
270
100 m
Juomasuo, Planview
Lithology
Sampling point
Albite rock
Chlorite rock
Ultra mafic
Sulphide lode or ore
Metasedimentary rock
Albite diabase
S > 1.0 %
20°0'0"E
25°0'0"E
30°0'0"E
70°0'0"N
68°0'0"N
66°0'0"N
64°0'0"N
Norway
Sweden
Russia
Juomasuo

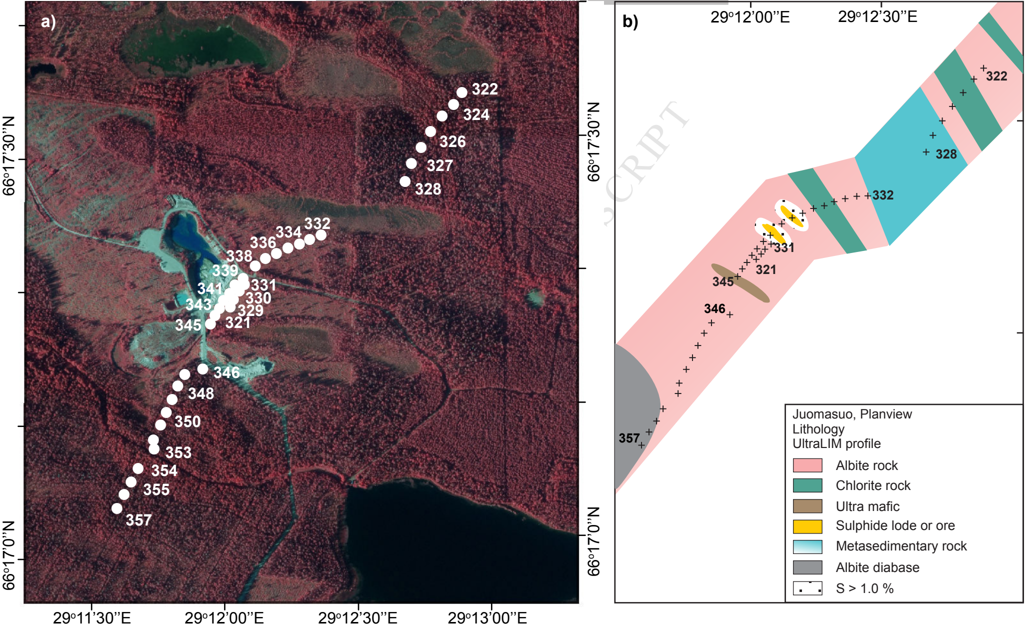
a)
322
324
326
327
328
332
334
336
338
339
331
341
330
343
329
345
321
346
348
350
353
354
355
357
66°17'30''N
66°17'0''N
29°11'30''E
29°12'00''E
29°12'30''E
29°13'00''E
b)
29°12'00''E
29°12'30''E
66°17'30''N
66°17'10''N
322
328
332
331
321
345
346
357
Juomasuo, Planview
Lithology
UltraLIM profile
Albite rock
Chlorite rock
Ultra mafic
Sulphide lode or ore
Metasedimentary rock
Albite diabase
S > 1.0 %

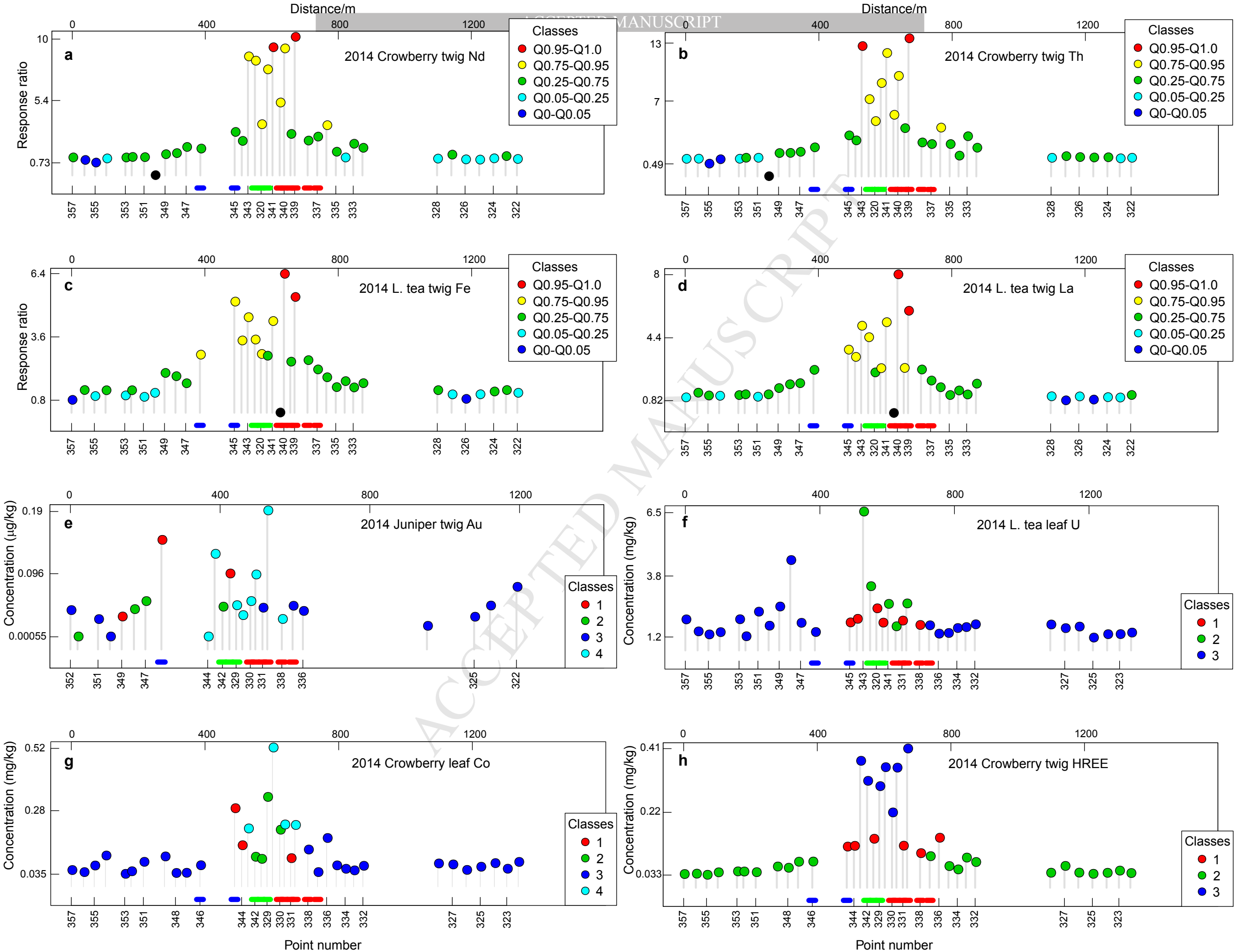

Distance/m
Response ratio
a
2014 Crowberry twig Nd
Classes
Q0.95-Q1.0
Q0.75-Q0.95
Q0.25-Q0.75
Q0.05-Q0.25
Q0-Q0.05
b
2014 Crowberry twig Th
c
2014 L. tea twig Fe
d
2014 L. tea twig La
e
2014 Juniper twig Au
Concentration (μg/kg)
f
2014 L. tea leaf U
Concentration (mg/kg)
g
2014 Crowberry leaf Co
h
2014 Crowberry twig HREE
Point number

Research highlights

- multi-elemental spatial anomaly patterns of Au and Co along with Fe, Th, U and rare earth elements in crowberry, Labrador tea and juniper tissue were observed over sub-outcropping lodes and deep (blind) Au-Co mineralizations
- evergreen species were most consistent in locating the mineralizations in early summer and late summer
- The vascular species used in this study are widely distributed over the pan-arctic and circum-boreal forests, thus demonstrating a great significance to mineral exploration of hydrothermal Au ores on the northern latitudes